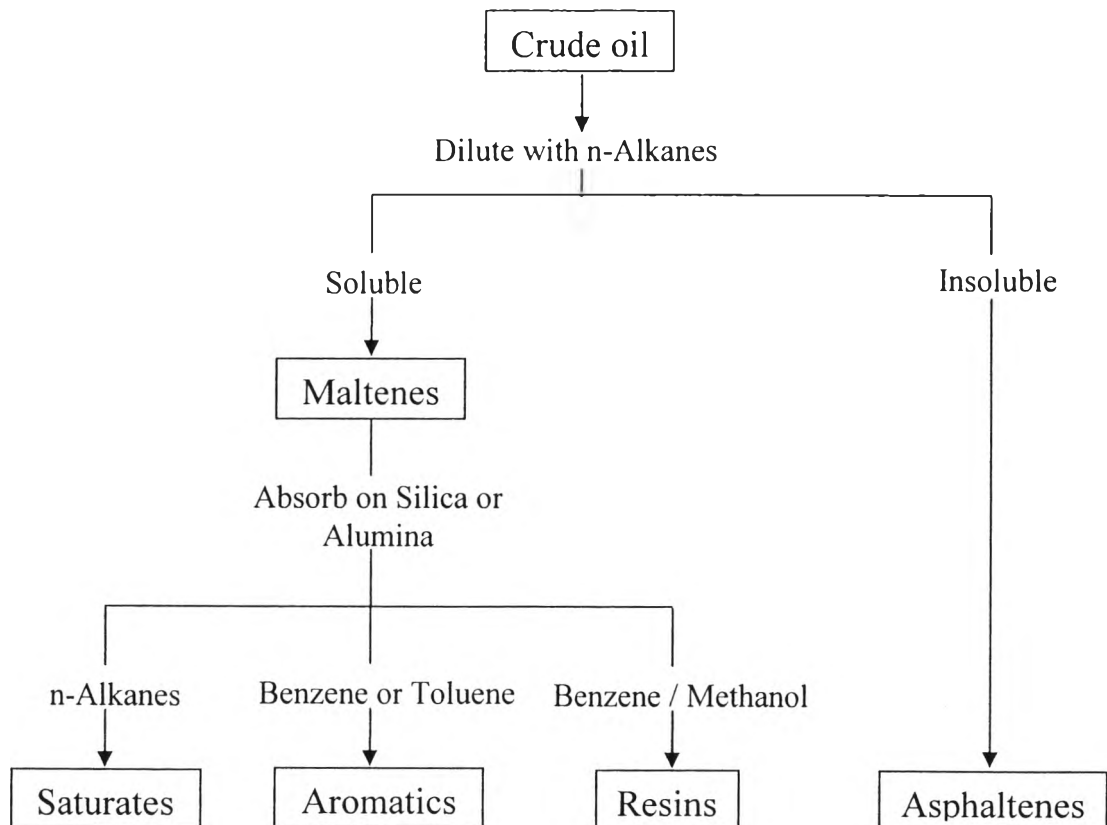




## CHAPTER II LITERATURE REVIEW

### 2.1 Crude Oil

Petroleum is a mixture of hydrocarbons and very complex organic compounds with Sulfur, Nitrogen, Oxygen, and other metallic elements such as nickel, vanadium, and iron (Hammami *et al.*, 2007). Crude oil is usually classified based upon the solubility class of each fraction using SARA separation technique. This technique divides crude oil into four major fractions: saturates, aromatics, resins, and asphaltenes.



**Figure 2.1** Schematic diagram of SARA separation (Speight, 2007).

In SARA fractionation, asphaltenes are defined as a fraction that precipitates while diluting crude oil with n-alkanes. The soluble fraction is called maltenes. Maltenes are then processed by absorption on silica or alumina adsorbents and eluted with solvents such as n-alkanes, benzene or toluene and benzene/methanol to recover saturates, aromatics and resins, respectively (Figure 2.1) (Speight, 2007).

## 2.2 Asphaltenes

Asphaltenes are the heaviest, and the most polar fraction of crude oil. Asphaltenes are believed to be composed of condensed aromatic cores with alkyl chains connected to them (island model). They are consisted of one or two polycyclic aromatic hydrocarbons (PAHs) per molecule as shown in Figure 2.2 (Durand *et al.*, 2010). Asphaltenes are defined as a solubility classes which are insoluble in n-alkanes, such as n-pentane and n-heptane, but soluble in aromatics such as toluene. They contain small amounts of heteroatoms (N, S and O) and trace metals (Ni, V and Fe). They are classified by the type of precipitant used for their precipitation. ASTM D2007-80 (1980) is a standard procedure that is used to quantify asphaltene content in crude oil by diluted with n-pentane or n-heptane in the volume ratio of 1:40 (crude oil : precipitant). If the precipitants are pentane and heptane, they are called pentane asphaltenes and heptane asphaltenes, respectively. Asphaltenes are observed as the brown and black powdery material (Speight, 2001; Nalwaya *et al.*, 1999).

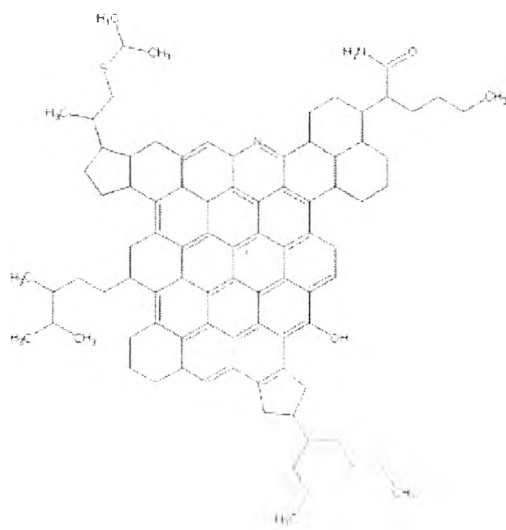


**Figure 2.2** Possible asphaltenes molecule structure (Durand *et al.*, 2010).

### 2.3 Asphaltene Precipitation

Asphaltenes can precipitate from crude oil due to change in temperature, pressure or composition. The precipitation of asphaltenes is usually induced by precipitant addition to simulate a real destabilization in wellbore. The amount of precipitant required to start asphaltene precipitation is defined as onset of precipitation (Pina *et al.*, 2006). The time that asphaltene particles require to reach a particle size of 0.5  $\mu\text{m}$  has defined the precipitation onset time (Maqbool *et al.*, 2009). Several techniques such as optical microscopy, viscosity, refractive index and light absorbance have been applied to detect asphaltene particles at onset point (Escobedo *et al.*, 1995; Wattana, 2004; Kraiwattanawong *et al.*, 2007). Most of these studies have conducted onset measurements on short time spans.

Angle *et al.* (2006) used optical microscope to examine the onset of precipitation on a longer time scale. They demonstrated that the growth of asphaltene precipitates can be a slow process depending on the amount of heptane added. Their experiments were conducted on crude oils mixed with toluene that is called model oil. Heptane was added to 10 wt% heavy oil at heptanes/toluene of 1.37 by weight to observe onset time and asphaltene particles were observed after 2 hours. They

showed that precipitation of asphaltenes does not happen instantaneously and depends both on time and precipitant concentration.

Toluene is a good solvent for asphaltenes and might hinder asphaltene precipitation. Therefore, it is not clear if the kinetics observed by Angle was due to toluene addition or not.

Maqbool *et al.* (2009) studied the kinetics of asphaltene precipitation in crude oils mixed with heptane. They observed that asphaltene precipitation is a time dependent process and particles can slowly grow over time to reach to a detectable size under microscopy (0.5  $\mu\text{m}$ ). Therefore the solution which initially seemed to be stable became unstable as time passed. They defined the time required to detect asphaltene instability after precipitant addition under microscopy as onset time (Figure 2.3) (Maqbool *et al.* (2009)). They showed that onset time is a strong function of heptane concentration and changes exponentially with it (Figure 2.4). The kinetic behavior is observed for different crude oils with different properties as shown in Figure 2.4. The work of Maqbool *et al.* (2009) challenges with previous works (Escobedo *et al.*, 1995; Wattana, 2004; Kraiwattanawong *et al.*, 2007) that precipitation of asphaltenes occur over a short period of time. Therefore, the precipitation of asphaltenes depends both on time and precipitant concentration.

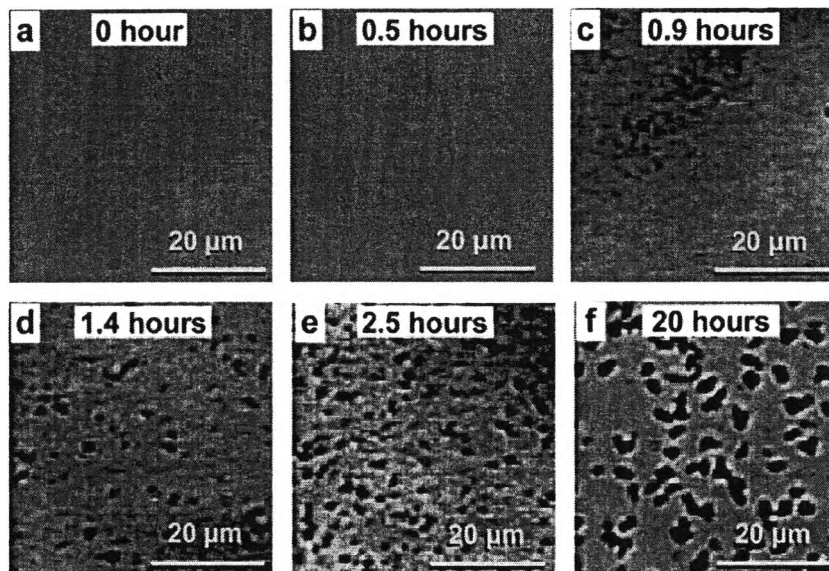


**Figure 2.3** Micrographs showing the time dependency of asphaltene precipitation for a crude-heptane mixture containing 50 vol% heptane and 50 vol% K-1 crude oil (Maqbool *et al.*, 2009).

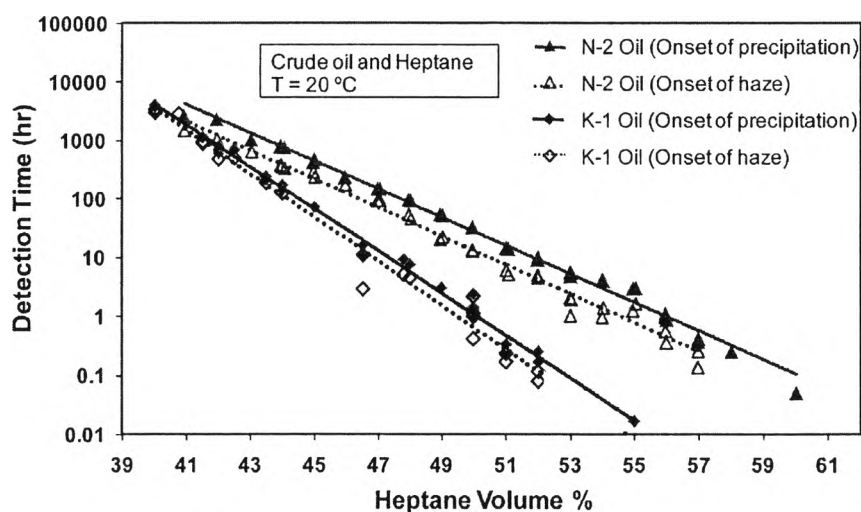


**Figure 2.4** Detection times for onset of precipitation and onset of haze at varying heptane concentrations using K-1 and N-2 crude oils (Maqbool *et al.*, 2009).

Maqbool *et al.* (2009) also developed a novel centrifugation technique and showed that yield of precipitated asphaltenes increases as a function of time at the

same heptane concentration (Figure 2.5). It was also shown that amount of precipitated asphaltenes increased by increasing precipitant concentration.

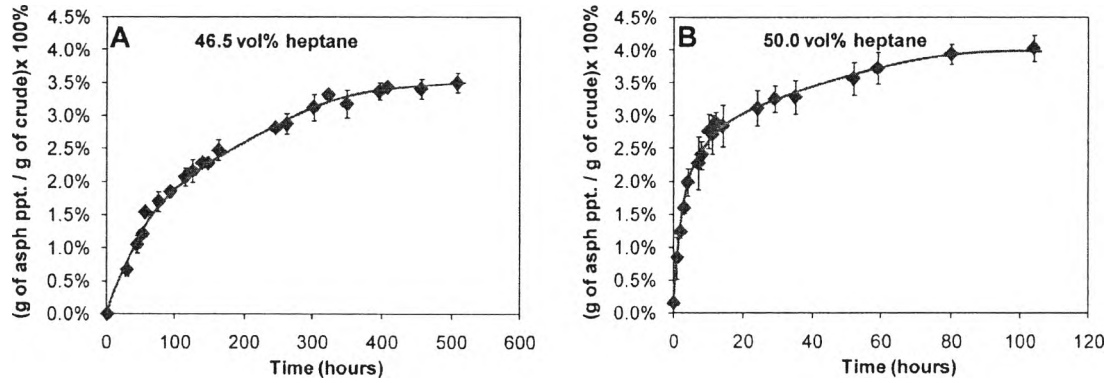


**Figure 2.5** Amount of asphaltenes precipitated as a function of time for K-1 crude oil at different heptane concentration: (a) 46.5 vol% heptane, (b) 50.0 vol% heptane (Maqbool *et al.*, 2009).

## 2.5 Modeling of the Kinetics of Asphaltene Precipitation by a Geometric Population Balance

As mentioned earlier, the asphaltene precipitation depends both on time and precipitant concentration. Maqbool (2011) have developed a model to describe the kinetic behavior of asphaltenes. The geometric population balance model is based on the assumption that asphaltenes get destabilized immediately after precipitant addition. The destabilized asphaltenes then aggregate and grow to larger sizes over time. The geometric population balance model is based on the Smoluchowski equation as shown in Eq (2.1). This equation shows the evolution of aggregates based on aggregation of particles of various sizes (Elimelech *et al.*, 1995).

$$\frac{dC_k}{dt} = \frac{1}{2} \sum_{\substack{i+j \rightarrow k \\ i=1}}^{i=k-1} K_{i,j} C_i C_j - C_k \sum_{j=1}^{\infty} K_{i,j} C_j \quad (2.1)$$

Where  $k = 1, 2, 3, \dots, N$  and  $N$  represents the number of aggregate units in the domain

$C_k$  is molar concentration of  $k$ -th aggregate ( $\text{kmol m}^{-3}$ )

$K_{i,j}$  is the collision kernel between aggregate sizes  $i$  and  $j$  ( $\text{m}^3 \text{kmol}^{-1} \text{s}^{-1}$ )

The first term on the right hand side is generation rate of  $k$ -th aggregates through binary collision of smaller aggregates. The second term is the consumption rate of  $k$ -th due to collision with other clusters.

The collision kernel ( $K_{i,j}$ ) in Eq (2.2) is a product of the collision frequency ( $\alpha_{i,j}$ ) and the collision efficiency ( $\beta$ ) (i.e.  $K_{i,j} = \beta \alpha_{i,j}$ ). The collision efficiency needs to be included because not every collision results in aggregation, it depends on interparticle interaction. The Brownian flocculation kernel that accounts for the aggregation of destabilized primary asphaltene particles starting from nanoaggregate sizes is used for collision kernel in this model. For Brownian flocculation, the collision frequency between aggregates  $i$  and  $j$  can be express as (Friedlander, 2000),

$$K_{i,j} = \frac{2R_g T (d_i + d_j)^2}{3\mu_m d_i d_j} \beta \quad (2.2)$$

Where  $d_i$  and  $d_j$  are the diameter of colliding aggregates  $i$  and  $j$  (m),  $\mu_m$  is viscosity of the medium ( $\text{kg m}^{-1} \text{s}^{-1}$ ),  $R_g$  is the universal gas constant ( $\text{J K}^{-1} \text{kmol}^{-1}$ ),  $T$  is the absolute temperature (K) and  $\beta$  is collision efficiency.

## 2.6 Crude Oil Properties

Oil industry has no heptane addition to destabilize asphaltenes but the asphaltene precipitation is leaded by changing in pressure, temperature and composition. The work of Maqbool *et al.* (2009) showed that the kinetics of asphaltene precipitation are important. It also showed that the precipitation rates of asphaltenes are not similar for different crude oils. The geometric population balance showed that aggregation rate of asphaltenes depends on interaction forces between asphaltene particles, diffusion rates and collision efficiency of unstable asphaltenes (Maqbool, 2011). To understand the properties that affect the asphaltene precipitation rate, the properties of crude oil such as viscosity and refractive index are measured in this study using rheometer and refractrometer, respectively.

### 2.6.1 Rheometer (Viscosity Measurement)

Rheometer is usually employed to measure flow and shear deformation of fluids. The properties that can be measured are dynamic quantity (i.e. a force, torque) and kinematic quantity (i.e. a velocity, shear rate, flow rate, time). The common types of rheometers are Capillary and Rotational Rheometers. The constant shear rate is used to find viscosity of Newtonian fluid like crude oil, therefore rotational rheometer with cone/plate configuration is used in this study. The fluid is placed between the plates of rheometer and the plates rotate or oscillate at same speed. The stress is applied to fluid and causes it to deform by rotation. The schematic of rotational rheometer is shown in Figure 2.6.

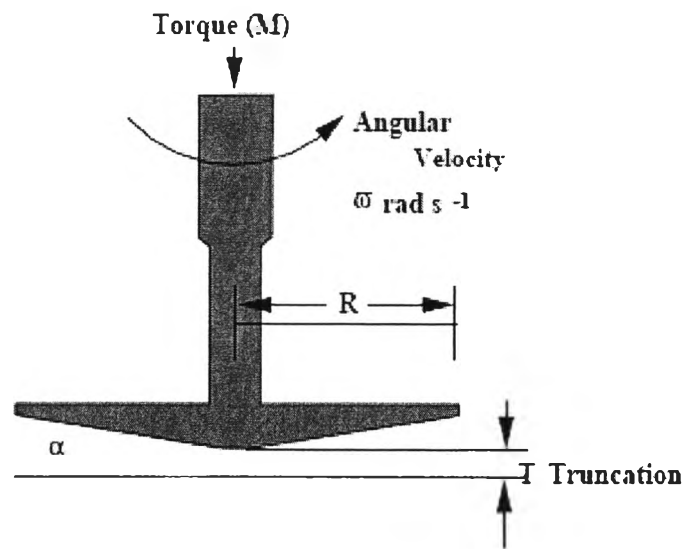


**Figure 2.6** Schematic of rotational rheometer (Cone/Plate) (Wikes, 2006).

Shear viscosity of fluid ( $\eta$ ) can be calculated using Eq (2.3) (Mezger, 2006).

$$\eta = \frac{\tau}{\dot{\gamma}} \quad (2.3)$$

Where  $\eta$  is shear viscosity (kg/ m s),  $\tau$  is shear stress (kg/ ms<sup>2</sup>) and  $\dot{\gamma}$  is shear rate (s<sup>-1</sup>)



Shear rate of fluid ( $\gamma$ ) can be calculated (Wilkes, 2006);

$$\gamma = \frac{v}{M} = \frac{\omega \cdot R}{R \cdot \tan \alpha} \quad (2.4)$$

Where  $v$  is velocity (m/s),  $M$  is torque (N m),  $\omega$  is angular velocity (rad/s),  $R$  is the radius of cone (m),  $\alpha$  is angle of cone (degree).

For small cone angle,  $\tan \alpha$  can be approximated around  $\alpha$ . Therefore,

$$\gamma = \frac{\omega}{\alpha} \quad (2.5)$$

Shear stress ( $\tau$ ) can be calculated using Eq (2.6) (Wilkes, 2006);

$$\tau = \frac{3M}{2\pi R^3} \quad (2.6)$$

Therefore, the shear viscosity can be calculated;

$$\eta = \frac{3 M \alpha}{2 \pi \omega R^3} \quad (2.7)$$

### 2.6.2 Refractometer (Refractive Index)

A refractometer is used to measure refractive index ( $n$ ) for calculating solubility parameter of crude oils. This method is done by shining a narrow light beam into a prism with the refractive sample at the bottom and measuring the angle at which total internal reflection occurs. Refractive index ( $n$ ) is a measure of speed of light through the substance and can be calculated using Eq 2.8 (Raymer, 2009).

$$n = \text{Speed of light in vacuum} / \text{Speed of light in substance} \quad (2.8)$$

RI is a function of temperature. RI decreases as temperature increases. The dependence of refractive index on the compositions in a mixture can be derived from the Clausius-Mosotti relation (Debye, 1929).

$$\alpha = \frac{3}{4\pi} \frac{M}{N_A \rho} \frac{(\epsilon - 1)}{(\epsilon + 2)} \quad (2.9)$$

Where  $\alpha$  is polarizability per molecule,  $M$  is molecular weight,  $N_0$  is the avogadro's number,  $\rho$  is density and  $\epsilon$  is dielectric constant.

From Maxwell's law, the dielectric constant ( $\epsilon$ ) at a specified frequency (visible or ultraviolet) is related to the refractive index ( $n$ ) (Atkins, 1998).

$$\epsilon = n^2 \quad (2.10)$$

Therefore, for an ideal binary mixture, a relationship between the refractive index function of the mixture and refractive index is (Wattana, 2004)

$$f(n) = \frac{n^2 - 1}{n^2 + 2} \quad (2.11)$$

The Hildebrand solubility parameter ( $\delta$ ) is a good indication of solubility that is used to estimate of the degree of interaction between materials (Hansen, 2007). Materials with similar values of solubility parameter are likely to be miscible. The Hildebrand solubility parameter is the square root of the cohesive energy density ( $C$ ) as shown in Eq (2.12) (Hansen, 2007).

$$\delta = \sqrt{C} \quad (2.12)$$

Wang (2000) showed that for liquids that London dispersion forces are more dominant than other van der Waals forces, refractive index function and solubility parameter are linearly correlated as shown in Eq (2.13).

$$\delta \text{ (MPa}^{1/2}\text{)} = 53.827 f(n) + 2.418 \quad (2.13)$$

## 2.7 Characterization of Asphaltenes

Better understanding about properties of asphaltenes precipitated under different conditions can help in identifying the properties responsible for asphaltene problems and therefore designing more effective remediation techniques. Properties of asphaltenes precipitated under different precipitant concentration have been investigated using different techniques in asphaltene literature. For example, the polarity based fractionations are applied to study the properties (e.g. aromaticity, functional groups, etc.) of polar fractions precipitated at different precipitant concentrations for solutions of asphaltenes dissolved in methyl chloride. It was shown that functional groups for different fractions were identical and no differences were identified by FTIR spectroscopy (Nalwaya *et al.*, 1999; Kaminski *et al.*, 2000).

It was also shown that metal contents (Fe, Ni and V) and heteroatoms increased by increasing polarity of asphaltenes. Wattana (2004) also demonstrated that there was an inverse relationship between solubility and polarity. In other words, asphaltenes with higher polarity had smaller solubility and higher tendency for precipitation. Buenrostro-Gonzalez *et al.* (2002) investigated the properties of precipitated asphaltenes in model oils. Their results showed that the heteroatoms content slightly decreased by increasing heptane concentration while the functional groups of asphaltenes remained unchanged. In addition,  $^1\text{H}$  NMR results showed that more stable fractions had smaller aromaticity. Trejo *et al.* (2004) also showed that the most unstable asphaltenes had the highest number of aromatic carbons and aromatic ring number in their structure. Martin *et al.* (2007) studied the properties of asphaltenes that were fractionated at different pentane concentration. They found that the second fraction (high pentane concentration) was more soluble than both the first (low pentane concentration) and the whole fractions at increasing heptane to toluene ratio. Moreover, the first fraction formed larger aggregates than the second fraction.

As mentioned earlier, the kinetics of asphaltene precipitation are important for understanding the problematic asphaltenes in oil industry, it is not clear what properties make some asphaltenes to precipitate earlier. Furthermore, the geometric population balance model assumed that all asphaltenes are destabilized rapidly after precipitant was added. Therefore the kinetics observed from microscopy is just due the time that takes for unstable asphaltenes to grow and reach to detectable size. It is also assumed the collision efficiency between unstable asphaltenes remains during aggregation process. If this assumption is correct, the properties of asphaltenes that precipitated at different time should be the same Maqbool (2011) tried to investigate the properties of asphaltenes precipitated at different times and precipitant concentrations for crude oil heptane mixtures. He found that asphaltenes that precipitated earlier, at a lower n-heptane concentration (Fraction #1 as shown in Figure 2.7(a)), had higher metal contents (Ni and V) than the asphaltenes precipitated at the highest n-heptane concentration (Fraction #5) as shown in Figure 2.7(b). However, metal contents do not significantly change among asphaltenes precipitated at different heptane concentrations. Therefore, no detectable difference is expected

on metal contents of the fractions precipitated at different times for constant heptane concentration.

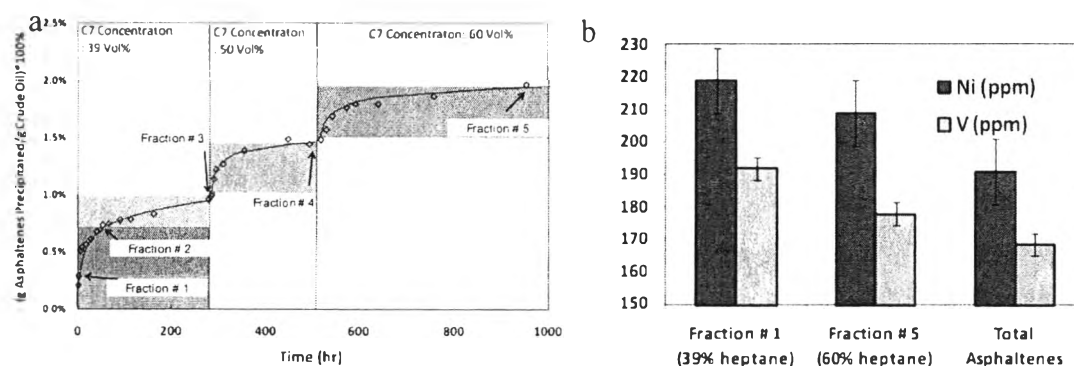


**Figure 2.7** (a) Characterization plot for GM2 oil (Maqbool, 2011)

(b) Comparison of the Ni and V concentrations in the three asphaltene fractions of GM2 oil (Maqbool, 2011).

All characterization studies discussed earlier have investigated the properties of precipitated asphaltenes as a function of precipitant concentration and not time. Therefore this study is focused on understanding the difference that makes some asphaltenes precipitate earlier than others. Small angle X-ray scattering (SAXS), nuclear magnetic resonance (NMR), elemental analyzer (EA) and inductively coupled plasma-mass spectroscopy (ICP-MS) are used to measure nanoaggregate size, structure parameters, heteroatom and metal contents in characterization experiments.

### 2.7.1 Small Angle X-Ray Scattering (SAXS)

SAXS is extensively used for the structural characterization of the dispersed particles in solution. Asphaltene molecules can scatter because of their high electron density. Their higher electron density is due to heteroatoms such as oxygen and nitrogen and metal compounds such as Ni and V. SAXS can be used in the range of nanoscale to measure the particle size, shape and polydispersity. The sample is hit by X-Ray primary beam and its pair correlation function is measured.

The scattering intensity is recorded as a function of the scattering vector as shown by equation 2.14 (Savvidis *et al.*, 2001).

$$q = 4\pi \sin(\theta)/\lambda \quad (2.14)$$

Where  $q$  is function of scattering vector,  $2\theta$  is the total scattering angle and  $\lambda$  is the X-ray wavelength.

For monodisperse particles, the intensity can be simplified as equation 2.15 (Savvidis *et al.*, 2001).

$$I(q) = S(q) F(q) \quad (2.15)$$

Where  $S(q)$  is structure factor and  $F(q)$  is form factor.

In dilute solution, structure factor is equal to one and the size of asphaltene aggregates can be estimated by Guinier Approximation (Eyssautier *et al.*, 2011);

$$I(q) = I_0 \exp\left(\frac{-(qR_g)^2}{3}\right) \quad (2.16)$$

where  $I(q)$  is scattering intensity at  $q$ ,  $I_0$  is scattering intensity at  $q=0$  and  $R_g$  is radius of gyration.

### 2.7.2 Nuclear Magnetic Resonance (NMR)

Nuclear Magnetic Resonance (NMR) is a technique that measures the absorption of electromagnetic radiation during transition between spin states of atoms and molecules in presence of magnetic field. Sample is placed in a magnetic field, and then all nuclei in sample are charged at a characteristic frequency in the radio frequency range of the electromagnetic spectrum. The resonance frequency, energy of the absorption and the intensity of the signal are proportional to the strength of the magnetic field. The resonance frequency can be used for defining the position of atom within a molecule and characterize the type of nucleus. Therefore, the bonding electrons create their own small magnetic field which modified the external magnetic field in nucleus. This variation is defined as chemical shift in parts per million.

Typically  $^1\text{H}$  NMR and  $^{13}\text{C}$  NMR are used for characterization of

asphaltenes dissolved in deuterated toluene ( $C_8D_8$ ), deuterated chloroform ( $CDCl_3$ ), deuterated methylene chloride, etc. The chemical shifts of solvent are shown in Table 2.1 (O'Neil *et al.*, 2006).

**Table 2.1** Chemical shift of solvent

Solvent	Chemical Shift (ppm)	
	$^1H$ NMR	$^{13}C$ NMR
Deuterated toluene	2.09, 6.98, 7.00, 7.09	20.4, 125.49, 128.33, 129.24, 137.24
Deuterated chloroform	7.24	77.23
Deuterated methylene chloride	5.32	54.00

$^{13}C$  and  $^1H$  NMR can provide information about asphaltene structure such as their aromaticity or average number of carbons per alky side chain. The  $^{13}C$  NMR spectra can be divided into two different integration domains to determine the fraction of aliphatic and aromatic carbons in structure of asphaltenes. The region of chemical shift in NMR spectra is shown in Table 2.2.

**Table 2.2** Assignments of chemical shifts in  $^{13}C$  NMR

Chemical Shift Range (ppm from TMS)	Assignment
10-60	$C_{al}$ : Aliphatic carbon
110-160	$C_{ar}$ : Aromatic Carbon

Aromaticity of asphaltenes can then be calculated from following (Peng *et al.*, 2010);

$$Aromaticity\ y(f_a) = \frac{C_{ar}}{C_{ar} + C_{al}} \quad (2.17)$$

Proton nuclear magnetic resonance ( $^1H$  NMR) can estimated average

number of carbon per alkyl side chain ( $n$ ) as shown in equation 2.18 (Peng *et al.*, 2010). It is the average length of alkyl side chain that connected to aromatic core of asphaltenes.

$$\text{Average number of carbon per alkyl side chain } (n) = \frac{H_{\alpha} + H_{\beta} + H_{\gamma}}{H_{\alpha}} \quad (2.18)$$

$H_{\alpha}$ ,  $H_{\beta}$  and  $H_{\gamma}$  are area under curve of  $^1\text{H}$  NMR spectra at chemical shifts as shown in Table 2.3.

**Table 2.3** Assignments of chemical shifts in  $^1\text{H}$  NMR

Chemical Shift Range (ppm from TMS)	Assignment
0.5-1.0	$H_{\gamma}$ : Hydrogen atoms of methyl groups of saturated compounds.
1.0-2.0	$H_{\beta}$ : Hydrogen atoms of methylene groups of saturated compounds.
2.0-4.0	$H_{\alpha}$ : Hydrogen atoms of the groups bonded next to aromatic rings, heteroatoms or carbonyl carbon atoms.
6.0-9.0	$H_{\text{ar}}$ : Aromatic hydrogen.

### 2.7.3 Elemental Analyzer (EA)

Elemental Analyzer is used to measure the amount of carbon, hydrogen and heteroatoms (N, O and S) in asphaltenes. EA analyses carbon, hydrogen and heteroatoms using combustion analysis which converts all organic and inorganic substances to combustion products such as carbon dioxide, water and nitric oxide. The masses of these combustion products are then used to calculate the composition of the sample (Pavia *et al.*, 2009).

### 2.7.4 Inductively Coupled Plasma-Mass Spectroscopy (ICP-MS)

Inductively Coupled Plasma-Mass Spectroscopy (ICP-MS) is used to measure metal contents. The solution of sample is sprayed into flowing argon and

passed into a torch at 10,000 °C. At high temperature, gas is atomized and ionized, forming plasma that provides a rich source of both excited and ionized atoms. The ion from plasma are extracted into a mass spectrometer and then separated on the basis of their mass to charge ratio. The ion signal is received by detector proportional to the concentration. The concentration of metal in sample can be determined through calibration with reference materials (Thomas, 2004).